

# PERTURBATIONS OF CIRCUIT EVOLUTION MATRICES WITH JORDAN BLOCKS

ALEXANDER FIGOTIN

**ABSTRACT.** In our prior studies we synthesized special circuits possessing evolution matrices that involve nontrivial Jordan blocks and the corresponding degenerate eigenfrequencies. The degeneracy of this type is sometimes referred to as exceptional point of degeneracy (EPD). The simplest of these circuits are composed just of two  $LC$ -loops coupled by a gyrator and they are of our primary interest here. These simple circuits when near an EPD state can be used for enhanced sensitivity applications. With that in mind we develop here a comprehensive perturbation theory for these simple circuits near an EPD as well way to assure their stable operation.

As to broader problem of numerical treatment of Jordan blocks and their perturbation we propose a few approaches allowing to detect the proximity to Jordan blocks.

## 1. INTRODUCTION

There is growing interest to electromagnetic system exhibiting Jordan eigenvector degeneracy, which is a degeneracy of the system evolution matrix when not only some eigenvalues, which often are frequencies, coincide but the corresponding eigenvectors coincide also. The degeneracy of this type is sometimes referred to as exceptional point of degeneracy (EPD), [Kato, II.1]. As to the Jordan canonical forms theory and its relations to differential equations we refer the reader to [Hale, III.4], [HorJohn, 3.1,3.2], [ArnODE, 25.4].

A particularly important class of applications of EPDs in sensing, [CheN]. [HHWGECK], [KNAC], [PeLiXu], [Wie], [Wie1]. The idea, in nutshell, of using EPDs for sensing is as follows. Suppose that sensing system is set to be at an EPD point before the measurement. Then when a sensor is engaged its signal of presumably small amplitude  $\epsilon$  perturbs the system altering its eigenfrequencies proportionally to  $\sqrt{\epsilon}$ . Since for small  $\epsilon$  its square root  $\sqrt{\epsilon}$  is much larger than  $\epsilon$  we get enhanced sensitivity.

We study here those aspects of the perturbation theory of Jordan blocks useful in detecting their presence and quantifying their proximity. Motivated by enhanced sensing applications we also develop detailed perturbation theory for the case of simple circuits as in Fig. 1.1 we introduced in [FigSynbJ]. The typical circuit of interest is composed of two  $LC$ -loops coupled with a gyrator, where  $L_j$  and  $C_j$  for  $j = 1, 2$  and  $G$  are respectively inductances and capacitances, that can be positive or negative, and the gyrator resistance. We refer the list of these parameters as the circuit parameters. We concisely review the relevant these circuits subjects from [FigSynbJ] in Section 2 and develop the perturbation for the circuits in Section 3.

An infinitesimally small transformation can be make a matrix with nontrivial Jordan structure completely diagonalizable. This fact complicates numerical assessment of the presence of nontrivial Jordan blocks as well as their utilization in application. In Section 6 we consider several approaches allowing to detect Jordan blocks numerically and quantify proximity to them.

---

*Key words and phrases.* Electric circuit, exceptional point of degeneracy (EPD), Jordan block, perturbations, instability, sensitivity.

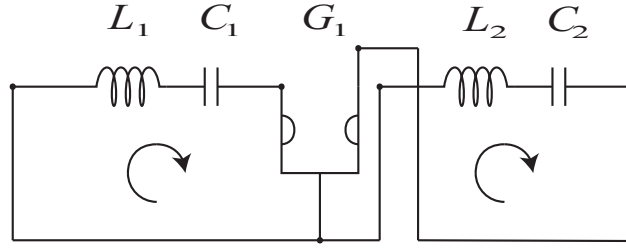


FIGURE 1.1. For particular choices of values for quantities  $L_1$ ,  $C_1$ ,  $L_2$ ,  $C_2$  and  $G_1$  the evolution matrix of this circuit develops EPDs, and its Jordan canonical form consists of exactly two Jordan blocks of the size two.

## 2. CIRCUIT AND ITS SPECIFICATIONS

We review concisely here properties of the circuit in Fig. 1.1 that we studied in [FigSynbJ, 4]. The circuit vector evolution equation and the corresponding eigenvalue problem are as follows

$$(2.1) \quad \partial_t \mathbf{q} = \mathcal{C} \mathbf{q}, \quad \mathcal{C} = \begin{bmatrix} 0 & 0 & 1 & 0 \\ 0 & 0 & 0 & 1 \\ -\frac{1}{L_1 C_1} & 0 & 0 & \frac{G_1}{L_1} \\ 0 & -\frac{1}{L_2 C_2} & -\frac{G_1}{L_2} & 0 \end{bmatrix}, \quad \mathbf{q} = \begin{bmatrix} q \\ \partial_t q \end{bmatrix},$$

$$(2.2) \quad (s\mathbb{I} - \mathcal{C}) \mathbf{q} = 0, \quad \mathbf{q} = \begin{bmatrix} q \\ sq \end{bmatrix}.$$

The characteristic polynomial associated with matrix  $\mathcal{C}$  defined by equations (2.1) and the corresponding characteristic equations are respectively

$$(2.3) \quad \chi(s) = \det \{s\mathbb{I} - \mathcal{C}\} = s^4 + \left( \xi_1 + \xi_2 + \frac{g}{L_1 L_2} \right) s^2 + \xi_1 \xi_2,$$

$$(2.4) \quad \chi(s) = s^4 + \left( \xi_1 + \xi_2 + \frac{g}{L_1 L_2} \right) s^2 + \xi_1 \xi_2 = 0,$$

where

$$(2.5) \quad \xi_1 = \frac{1}{L_1 C_1}, \quad \xi_2 = \frac{1}{L_2 C_2}, \quad g = G_1^2.$$

We refer to positive  $g = G_1^2$  in equations (2.5) as the *gyration parameter*. Notice that using parameters in equations (2.5) we can recast the companion matrix  $\mathcal{C}$  defined by equations (2.1) and its characteristic function  $\chi(s)$  as in equation (2.4) as follows

$$(2.6) \quad \mathcal{C} = \begin{bmatrix} 0 & 0 & 1 & 0 \\ 0 & 0 & 0 & 1 \\ -\xi_1 & 0 & 0 & \frac{G_1}{L_1} \\ 0 & -\xi_2 & -\frac{G_1}{L_2} & 0 \end{bmatrix},$$

$$(2.7) \quad \chi(s) = \chi_h = h^2 + \left( \xi_1 + \xi_2 + \frac{g}{L_1 L_2} \right) h + \xi_1 \xi_2, \quad h = s^2.$$

The solutions to the quadratic equation  $\chi_h = 0$  are

$$(2.8) \quad h_{\pm} = \frac{-\left( \xi_1 + \xi_2 + \frac{g}{L_1 L_2} \right) \pm \sqrt{\Delta_h}}{2},$$

where

$$(2.9) \quad \Delta_h = \frac{g^2}{L_1^2 L_2^2} + \frac{2(\xi_1 + \xi_2)g}{L_1 L_2} + (\xi_1 - \xi_2)^2$$

is the discriminant of the quadratic polynomial  $\chi_h$  (2.7). The corresponding four solutions  $s$  to the characteristic equation (2.4), that is the eigenvalues, are

$$(2.10) \quad s = \pm\sqrt{h_+}, \pm\sqrt{h_-},$$

where  $h_{\pm}$  satisfy equations (2.8).

Notice that the eigenvalue degeneracy condition turns into equation  $\Delta_h = 0$  which is equivalent to

$$(2.11) \quad L_1^2 L_2^2 \Delta_h = g^2 + 2(\xi_1 + \xi_2)gL_1 L_2 + (\xi_1 - \xi_2)^2 L_1^2 L_2^2 = 0.$$

Equation (2.11) evidently is a constraint on the circuit parameters which is a quadratic equation for  $g$ . Being given the circuit coefficients  $\xi_1$ ,  $\xi_2$ ,  $L_1$  and  $L_2$  this quadratic in  $g$  equation has exactly two solutions

$$(2.12) \quad g_{\delta} = \left(-\xi_1 - \xi_2 + 2\delta\sqrt{\xi_1\xi_2}\right) L_1 L_2, \quad \delta = \pm 1.$$

We refer to  $g_{\delta}$  in equations (2.12) as *special values of the gyration parameter  $g$* . For the two special values  $g$  we get from equations (2.8) the corresponding two degenerate roots

$$(2.13) \quad h = -\frac{\xi_1 + \xi_2 + \frac{g}{L_1 L_2}}{2} = \pm\sqrt{\xi_1\xi_2}.$$

Since  $G_1$  is real then  $g = G_1^2$  is real as well. The expression (2.12) for  $g$  is real-valued if and only if

$$(2.14) \quad \xi_1\xi_2 > 0, \text{ or equivalently } \frac{\xi_1}{|\xi_1|} = \frac{\xi_2}{|\xi_2|} = \sigma,$$

where we introduced a binary variable  $\sigma$  taking values  $\pm 1$ . We refer to  $\sigma$  as the *circuit sign index*. Relations (2.14) imply in particular that the equality of signs  $\text{sign}\{\xi_1\} = \text{sign}\{\xi_2\}$  is a necessary condition for the eigenvalue degeneracy condition  $\Delta_h = 0$  provided that  $g$  has to be real-valued.

It follows then from relations (2.12) and (2.14) that the special values of the gyration parameter  $g_{\delta}$  can be recast as

$$(2.15) \quad g_{\delta} = -\sigma \left(\sqrt{|\xi_1|} + \delta\sqrt{|\xi_2|}\right)^2 L_1 L_2, \quad \delta = \pm 1,$$

where  $\sqrt{\xi} > 0$  for  $\xi > 0$ . Recall that  $g = G_1^2 > 0$  and to provide for that we must have in right-hand side of equations (2.15)

$$(2.16) \quad -\sigma L_1 L_2 > 0, \text{ or equivalently } \frac{L_1 L_2}{|L_1 L_2|} = -\sigma.$$

Relations (2.14) and (2.16) on the signs of the involved parameters can be combined into the *circuit sign constraints*

$$(2.17) \quad \text{sign}\{\xi_1\} = \text{sign}\{\xi_2\} = -\text{sign}\{L_1 L_2\} = \text{sign}\{\sigma\}.$$

Notice that the sign constraints (2.17) involving the circuit index  $\sigma$  defined by (2.14) are necessary for the eigenvalue degeneracy condition  $\Delta_h = 0$ . Combing equations (2.15) and (2.16) we obtain

$$(2.18) \quad g_{\delta} = \left(\sqrt{|\xi_1|} + \delta\sqrt{|\xi_2|}\right)^2 |L_1 L_2|, \quad \delta = \pm 1, \text{ assuming the circuit sign constraints.}$$

Since  $g = G_1^2 > 0$  the special values of the gyrator resistance  $\dot{G}_1$  corresponding to the special values  $g_\delta$  as in equation (2.18) are

$$(2.19) \quad \dot{G}_1 = \sigma_1 \sqrt{g_\delta} = \sigma_1 \left( \sqrt{|\xi_1|} + \delta \sqrt{|\xi_2|} \right) \sqrt{|L_1 L_2|}, \text{ assuming the circuit sign constraints,}$$

where the binary variable  $\sigma_1$  takes values  $\pm 1$ .

Using representation (2.18) for  $g_\delta$  under the circuit sign constraints (2.17) we can recast the expression for the degenerate root  $\dot{h}$  in equations (2.13) as follows

$$(2.20) \quad h_\delta = \sigma \delta \sqrt{|\xi_1|} \sqrt{|\xi_2|}, \text{ for } g = g_\delta = \left( \sqrt{|\xi_1|} + \delta \sqrt{|\xi_2|} \right)^2 |L_1 L_2|, \quad \delta = \pm 1,$$

where  $\sigma$  is the circuit sign index defined by equations (2.14) and  $\sqrt{\xi} > 0$  for  $\xi > 0$ .

One the principal results regarding the circuit in Fig. 1.1 is as follows [FigSynbJ].

**Theorem 1** (Jordan form under degeneracy). *Let the circuit be as depicted in Fig. 1.1 and let all its parameters  $L_1, C_1, L_2, C_2$  and  $G_1$  be real and non-zero. Then the companion matrix  $\mathcal{C}$  satisfying equations (2.1) and (2.6) has the Jordan form*

$$(2.21) \quad \mathcal{J} = \begin{bmatrix} s_0 & 1 & 0 & 0 \\ 0 & s_0 & 0 & 0 \\ 0 & 0 & -s_0 & 1 \\ 0 & 0 & 0 & -s_0 \end{bmatrix},$$

if and only if the circuit parameters satisfy the degeneracy conditions as in equation (2.11). Then for  $g = g_\delta$  we have

$$(2.22) \quad h_\delta = \sigma \delta \sqrt{|\xi_1|} \sqrt{|\xi_2|}, \text{ for } g = g_\delta = \left( \sqrt{|\xi_1|} + \delta \sqrt{|\xi_2|} \right)^2 |L_1 L_2|,$$

$$(2.23) \quad \pm s_0 = \pm \sqrt{\sigma \delta \sqrt{|\xi_1|} \sqrt{|\xi_2|}}, \text{ for } g = g_\delta = \left( \sqrt{|\xi_1|} + \delta \sqrt{|\xi_2|} \right)^2 |L_1 L_2|,$$

where  $\sqrt{\xi} > 0$  for  $\xi > 0$ ,  $\delta = \pm 1$  and  $\sigma$  is the circuit sign index defined by equations (2.14). According to formula (2.23) degenerate eigenvalues  $\pm s_0$  depend on the product  $\sigma \delta$  and  $|\xi_1|, |\xi_2|$  and consequently they are either real or pure imaginary depending on whether  $\delta = \sigma$  or  $\delta = -\sigma$ .

Notice that in the special case when  $|\xi_1| = |\xi_2|$  the parameter  $g_\delta$  takes only one non-zero value, namely

$$(2.24) \quad g = g_1 = 4 |\xi_1| |L_1 L_2|, \quad L_1 L_2 = -\sigma |L_1 L_2|,$$

whereas  $g_{-1} = 0$  which is inconsistent with our assumption  $G_1 \neq 0$ . Evidently for  $g = 0$  the circuit breaks into two independent LC-circuits and in this case the relevant Jordan form is a diagonal  $4 \times 4$  matrix with eigenvalues  $\pm \sqrt{\xi_1}$  and  $\pm \sqrt{\xi_2}$ .

*Remark 2* (instability and marginal stability). Notice according to formula (2.23) degenerate eigenvalues  $\pm s_0$  are real for  $\delta = \sigma$  and hence they correspond to exponentially growing and decaying in time solutions indicating instability. For  $\delta = -\sigma$  the degenerate eigenvalues  $\pm s_0$  are pure imaginary corresponding to oscillatory solutions indicating that there is at least marginal stability.

To get a graphical illustration for the circuit complex-valued eigenvalues as functions of the gyration parameter  $g$  we use the following data

$$(2.25) \quad |\xi_1| = 1, \quad |\xi_2| = 2, \quad |L_1| = 1, \quad |L_2| = 2, \quad \sigma = 1,$$

and that corresponds to

$$(2.26) \quad \xi_1 = 1, \quad \xi_2 = 2, \quad L_1 = \pm 1, \quad L_2 = \mp 2.$$

It follows then from representation (2.18) that the corresponding special values  $g_\delta$  are

$$(2.27) \quad g_{-1} = 2 \left(1 - \sqrt{2}\right)^2 \cong 0.3431457498, \quad g_1 = 2 \left(1 + \sqrt{2}\right)^2 \cong 11.65685425.$$

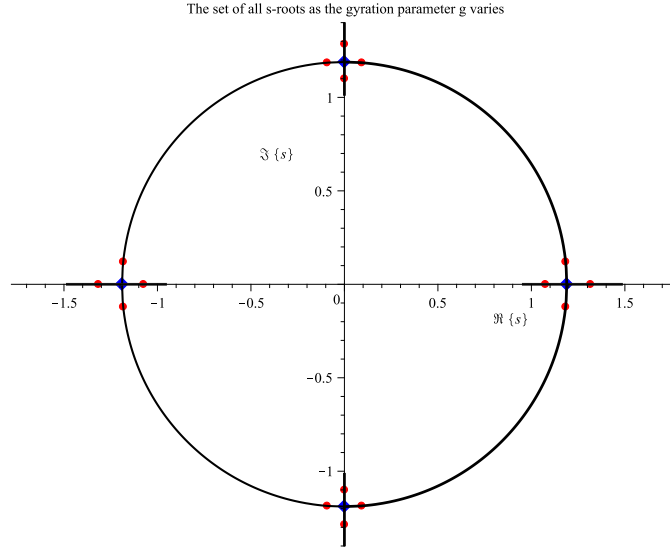


FIGURE 2.1. The plot shows the set  $S_{\text{eig}}$  of all complex valued eigenvalues  $s$  defined by equations (2.10) for the data in equations (2.25), (2.26) when the gyration parameter  $g$  varies in interval containing special values  $g_{-1}$  and  $g_1$  defined in relations (2.27). The horizontal and vertical axes represent the real and the imaginary parts  $\Re\{s\}$  and  $\Im\{s\}$  of eigenvalues  $s$ .  $S_{\text{eig}}$  consists of the circle centered in the origin of radius  $\sqrt[4]{|\xi_1||\xi_2|}$  and four intersecting its intervals lying on real and imaginary axes. The circular part of the set  $S_{\text{eig}}$  corresponds to all eigenvalues for  $g_{-1} \leq g \leq g_1$ . The degenerate eigenvalues  $\pm s_0$  corresponding to  $g_{-1}$  and  $g_1$  and defined by equations (2.23) are shown as solid diamond (blue) dots. Two of them are real, positive and negative, numbers and another two are pure imaginary, with positive and negative imaginary parts. The 16 solid circular (red) dots are associated with 4 quadruples of eigenvalues corresponding to 4 different values of the gyration parameter  $g$  chosen to be slightly larger or smaller than the special values  $g_{-1}$  and  $g_1$ . Let us take a look at any of the degenerate eigenvalues identified by solid diamond (blue) dots. If  $g$  is slightly different from its special values  $g_{-1}$  and  $g_1$  then each degenerate eigenvalue point splits into a pair of points identified by solid circular (red) dots. They are either two real or two pure imaginary points if  $g$  is outside the interval  $[g_{-1}, g_1]$ , or alternatively they are two points lying on the circle, if  $g$  is inside the interval  $[g_{-1}, g_1]$ .

To explain the rise of the circular part of the set  $S_{\text{eig}}$  in Fig. 2.1 we recast the characteristic equation (2.7) as follows

$$(2.28) \quad H + \frac{1}{H} = R, \quad R = \frac{\sigma}{\sqrt{|\xi_1||\xi_2|}} \left[ \frac{g}{|L_1||L_2|} - (|\xi_1| + |\xi_2|) \right], \quad H = \frac{h}{\sqrt{|\xi_1||\xi_2|}}.$$

Notice that

$$(2.29) \quad R = 2\delta\sigma, \text{ for } g = g_\delta = \left( \sqrt{|\xi_1|} + \delta\sqrt{|\xi_2|} \right)^2 |L_1L_2|, \quad \delta = \pm 1,$$

where  $\sigma = \pm 1$  is the circuit sign index. Since  $R$  depends linearly on  $g$  relations (2.28) and (2.29) imply

$$(2.30) \quad |R| \leq 2, \text{ for } g_{-1} \leq g \leq g_1; \quad |R| > 2, \text{ for } g < g_{-1} \text{ and } g > g_1.$$

It is an elementary fact that solutions  $H$  to equation (2.28) satisfy the following relations:

$$(2.31) \quad H = \exp \{i\theta\}, \text{ for } |R| \leq 2, \text{ and } \cos(\theta) = \frac{R}{2}, \quad 0 \leq \theta \leq \pi,$$

$$(2.32) \quad H > 0, \text{ for } R > 2, \text{ and } H < 0, \text{ for } R < -2.$$

It is also evident from the form of equation (2.28) that if  $H$  is its solution then  $H^{-1}$  is a solution as well, that is the two solutions to equation (2.28) always come in pairs of the form  $\{H, H^{-1}\}$ .

Since the eigenvalues  $s$  satisfy  $s = \pm\sqrt{h}$  the established above properties of  $h = \sqrt{|\xi_1||\xi_2|}H$  can recast for  $s$  as follows.

**Theorem 3** (quadruples of eigenvalues). *For every  $g > 0$  every solution  $s$  to the characteristic equation (2.4) is of the form (2.10) and the number of solutions is exactly four counting their multiplicity. Every such a quadruple of solutions is of the following form*

$$(2.33) \quad \left\{ s, \frac{\sqrt{|\xi_1||\xi_2|}}{s}, -s, -\frac{\sqrt{|\xi_1||\xi_2|}}{s} \right\},$$

where  $s$  is a solution to the characteristic equation (2.4). Then for  $g_{-1} \leq g \leq g_1$  the quadruple of solutions belongs to the circle  $|s| = \sqrt[4]{|\xi_1||\xi_2|}$  such that

$$(2.34) \quad s = \delta_1 \sqrt[4]{|\xi_1||\xi_2|} \exp \{i\delta_2\theta\}, \quad \cos(\theta) = \frac{R}{2}, \quad 0 \leq \theta \leq \pi, \quad \delta_1, \delta_2 = \pm 1,$$

where  $R$  is defined in relations (2.28). If  $g < g_{-1}$  or  $g > g_1$  the quadruple of solutions consists of either real numbers and pure imaginary numbers depending if  $R > 2$  or  $R < -2$  respectively. In view of relations (2.28) and  $s = \pm\sqrt{h}$  where  $h = \sqrt{|\xi_1||\xi_2|}H$  every quadruple of solutions as in expression (2.33) is invariant with respect to the complex conjugation transformation.

The following remark discusses in some detail the transition of eigenvalues lying on the circle  $|s| = \sqrt[4]{|\xi_1||\xi_2|}$  having non-zero real and imaginary parts into either real or pure imaginary numbers as the value of the gyration parameter  $g$  passes through its special values  $g_{-1}$  or  $g_1$  at which the eigenvalues degenerate.

*Remark 4* (transition at degeneracy points). According to formula (2.23) there is total of four degenerate eigenvalues  $\pm s_0$ , namely  $\pm\sqrt[4]{|\xi_1||\xi_2|}$  and  $\pm i\sqrt[4]{|\xi_1||\xi_2|}$  (depicted as solid diamond (blue) dots in Fig. 2.1) that are associated with the two special values of the gyration parameter  $g_{\pm 1} = \left(\sqrt{|\xi_1|} \pm \sqrt{|\xi_2|}\right)^2 |L_1 L_2|$ . For any value of the gyration parameter  $g$  different than its two special values there are exactly four distinct eigenvalues  $s$  forming a quadruple as in expression (2.33). If  $g_{-1} < g < g_1$  and  $g$  gets close to either  $g_{-1}$  or  $g_1$  the corresponding four distinct eigenvalues on the circle  $|s| = \sqrt[4]{|\xi_1||\xi_2|}$  get close to either  $\pm\sqrt[4]{|\xi_1||\xi_2|}$  or  $\pm i\sqrt[4]{|\xi_1||\xi_2|}$  as depicted in Fig. 2.1) by solid circle (red) dots. As  $g$  approaches the special values  $g_{-1}$  or  $g_1$ , reaches them and gets out of the interval  $[g_{-1}, g_1]$  the corresponding solid circle (red) dots approach the relevant points  $\pm\sqrt[4]{|\xi_1||\xi_2|}$  or  $\pm i\sqrt[4]{|\xi_1||\xi_2|}$ , merge at them and then split again passing to respectively real and imaginary axes as illustrated by Fig. 2.1.

## 3. PERTURBATION THEORY FOR THE CIRCUIT

We develop here the perturbation theory for the circuit in Fig. 1.1 at its EPD point. The circuit and its relevant properties are reviewed in Section 2. Our primary case of interest here is when the circuit parameters satisfy

$$(3.1) \quad \xi_1, \xi_2, -L_1 L_2 > 0, \quad R \cong -2,$$

implying in view of the sign constraints (2.5) and relations (2.29) the following relations for the circuit parameters at the EPD point:

$$(3.2) \quad \sigma = 1, \quad \delta = -1; \quad R = 2\delta\sigma = -2, \text{ for } g = g_{-1} = -\left(\sqrt{\xi_1} - \sqrt{\xi_2}\right)^2 L_1 L_2.$$

Then the frequencies

$$(3.3) \quad \omega_1 = \frac{1}{\sqrt{L_1 C_1}} = \sqrt{\xi_1} > 0, \quad \omega_2 = \frac{1}{\sqrt{L_2 C_2}} = \sqrt{\xi_2} > 0.$$

associated with the circuit  $LC$ -loops are real, and also according to Theorem 3 and Remark 4 the circuit degenerate frequency at the EPD is

$$(3.4) \quad \dot{\omega} = \sqrt[4]{\xi_1 \xi_2} = \sqrt{\omega_1 \omega_2} > 0,$$

where  $\xi_1, \xi_2$  and  $\omega_1, \omega_2$  are the values of the parameters at the EPD point. Equation (3.4) indicates that the circuit at the EPD is at least marginally stable explaining why this EPD point satisfying equations (3.1) and (3.2) is of our primary interest.

Let us turn now to the characteristic equation (2.28). This equation under conditions (3.1) and in view of relations (3.2) takes here the form

$$(3.5) \quad H + \frac{1}{H} = -2 - r, \\ r = \frac{1}{\sqrt{\xi_1 \xi_2}} \left[ \frac{g}{L_1 L_2} + (\xi_1 + \xi_2) \right] + 2, \quad H = \frac{h}{\sqrt{\xi_1 \xi_2}},$$

where

$$(3.6) \quad r = 0, \text{ for } g = g_{-1} = -\left(\sqrt{\xi_1} - \sqrt{\xi_2}\right)^2 L_1 L_2.$$

Let us consider now a fixed EPD point with the circuit parameters

$$(3.7) \quad \dot{L}_j, \quad \dot{C}_j, \quad j = 1, 2; \quad \dot{g} = -\left(\sqrt{\dot{\xi}_1} - \sqrt{\dot{\xi}_2}\right)^2 \dot{L}_1 \dot{L}_2$$

and its perturbation of the form

$$(3.8) \quad L_j = \dot{L}_j (1 + \Delta(L_j) \epsilon), \quad C_j = \dot{C}_j (1 + \Delta(C_j) \epsilon), \quad j = 1, 2; \quad g = \dot{g} (1 + \Delta(g) \epsilon),$$

where  $\epsilon$  is a small real-valued parameter and  $\Delta(L_j)$ ,  $\Delta(C_j)$  and  $\Delta(g)$  are real-valued coefficients that weight the variation of the . We often will assume that it is only one of these coefficients differs from zero.

Note that if  $r$  is small then the two solutions  $H$  to equation (3.5) satisfy the following asymptotic formula

$$(3.9) \quad H = -1 \pm \sqrt{r} + O(r), \quad r \rightarrow 0.$$

For the circuit parameters as in equations (3.8) we have

$$(3.10) \quad r = \Delta(R) \epsilon + O(\epsilon^2), \quad \epsilon \rightarrow 0,$$

where

$$(3.11) \quad \Delta(R) = \left( \frac{\sqrt{\xi_1}}{\sqrt{\xi_2}} - 1 \right) \Delta_1(R) + \left( \frac{\sqrt{\xi_2}}{\sqrt{\xi_1}} - 1 \right) \Delta_2(R),$$

$$\Delta_1(R) = \Delta(L_2) - \Delta(C_1) + \Delta(g), \quad \Delta_2(R) = \Delta(L_1) - \Delta(C_2) + \Delta(g).$$

Using equation  $H = \frac{h}{\sqrt{\xi_1 \xi_2}}$  and taking the square root of the two solutions  $H$  defined by equations (3.9) and (3.10) we obtain after elementary algebraic transformation four solutions  $s$  for the original characteristic equation (2.4), (2.5)

$$(3.12) \quad s = i\omega = i\sqrt[4]{\dot{\xi}_1 \dot{\xi}_2} \left( 1 \pm \frac{1}{2} \sqrt{\Delta(R)\epsilon} + O(\epsilon) \right), \quad -i\sqrt[4]{\dot{\xi}_1 \dot{\xi}_2} \left( 1 \pm \frac{1}{2} \sqrt{\Delta(R)\epsilon} + O(\epsilon) \right), \quad \epsilon \rightarrow 0,$$

where coefficient  $\Delta(R)$  satisfies representation (3.11). Evidently the above solutions are pure imaginary if  $\Delta(R)\epsilon > 0$ .

Equations (3.12) and (3.4) imply the following expressions for the two split frequencies and their relative difference

$$(3.13) \quad \omega_{\pm} = \sqrt[4]{\dot{\xi}_1 \dot{\xi}_2} \left( 1 \pm \frac{1}{2} \sqrt{\Delta(R)\epsilon} + O(\epsilon) \right) = \dot{\omega} \left( 1 \pm \frac{1}{2} \sqrt{\Delta(R)\epsilon} + O(\epsilon) \right),$$

$$(3.14) \quad \frac{\omega_+ - \omega_-}{\dot{\omega}} = \sqrt{\Delta(R)\epsilon} + O(\epsilon).$$

We refer to the difference  $\omega_+ - \omega_-$  as *frequency split* and to  $\frac{\omega_+ - \omega_-}{\dot{\omega}}$  as *relative frequency split*.

Using frequencies  $\omega_1$  and  $\omega_2$  defined by equations (3.3) the representation (3.11) for  $\Delta(R)$  can be recast as

$$(3.15) \quad \Delta(R) = \left( \frac{\omega_1}{\omega_2} - 1 \right) \Delta_1(R) + \left( \frac{\omega_2}{\omega_1} - 1 \right) \Delta_2(R),$$

$$\Delta_1(R) = \Delta(C_1) - \Delta(L_2) - \Delta(g), \quad \Delta_2(R) = \Delta(C_2) - \Delta(L_1) - \Delta(g).$$

Notice that the following elementary inequality holds

$$(3.16) \quad \xi - 1 > 1 - \frac{1}{\xi} = \frac{\xi - 1}{\xi}, \quad \text{for } \xi > 1,$$

readily implying

$$(3.17) \quad \left| \frac{\omega_1}{\omega_2} - 1 \right| > \left| \frac{\omega_2}{\omega_1} - 1 \right| \quad \text{if } \omega_1 > \omega_2.$$

Notice also the equation (3.4) for the circuit degenerate frequency  $\dot{\omega}$  at the EPD implies

$$(3.18) \quad \omega_1 > \dot{\omega} > \omega_2 \quad \text{if } \omega_1 > \omega_2.$$

Assuming that the only circuit parameter that varies is capacitance  $C_1$  and that its relative change  $\Delta(C_1) = \frac{C_1 - \dot{C}_1}{C_1}$  is small we obtain from equations (3.14) for  $\epsilon = 1$

$$(3.19) \quad \frac{\omega_+ - \omega_-}{\dot{\omega}} \cong \sqrt{-\left( \frac{\omega_1}{\omega_2} - 1 \right) \Delta(C_1)} = \sqrt{-\left( \frac{\omega_1}{\omega_2} - 1 \right) \frac{C_1 - \dot{C}_1}{C_1}}.$$



Similarly under the assumption of smallness of the relative change of the varying variables  $L_1$ ,  $C_2$ ,  $L_2$ , and  $g$  we get respectively the following relations

$$(3.20) \quad \frac{\omega_+ - \omega_-}{\dot{\omega}} \cong \sqrt{\left(\frac{\omega_2}{\omega_1} - 1\right) \Delta(L_1)} = \sqrt{\left(\frac{\omega_2}{\omega_1} - 1\right) \frac{L_1 - \dot{L}_1}{\dot{L}_1}},$$

$$(3.21) \quad \frac{\omega_+ - \omega_-}{\dot{\omega}} \cong \sqrt{-\left(\frac{\omega_2}{\omega_1} - 1\right) \Delta(C_2)} = \sqrt{-\left(\frac{\omega_2}{\omega_1} - 1\right) \frac{C_2 - \dot{C}_2}{\dot{C}_2}},$$

$$(3.22) \quad \frac{\omega_+ - \omega_-}{\dot{\omega}} \cong \sqrt{\left(\frac{\omega_1}{\omega_2} - 1\right) \Delta(L_2)} = \sqrt{\left(\frac{\omega_1}{\omega_2} - 1\right) \frac{L_2 - \dot{L}_2}{\dot{L}_2}},$$

$$(3.23) \quad \frac{\omega_+ - \omega_-}{\dot{\omega}} \cong \sqrt{\left(2 - \frac{\omega_1}{\omega_2} - \frac{\omega_2}{\omega_1}\right) \Delta(g)} = \sqrt{\left(2 - \frac{\omega_1}{\omega_2} - \frac{\omega_2}{\omega_1}\right) \frac{g - \dot{g}}{\dot{g}}}.$$

Notice that for the quantities under the sign of square root in relations (3.19)-(3.23) to be positive the relevant relative changes of the circuit parameters must have proper signs.

In view of equations (3.12), (3.15) and inequality (3.16) as well as relations (3.19)-(3.23) the following statement holds.

**Theorem 5** (rate of change of the eigenfrequencies). *Suppose that  $\omega_1 > \omega_2$  where the indicated frequencies are defined by equations (3.3). Then the rate of change of the eigenfrequencies defined by equation (3.12) for small  $\epsilon$  is higher as  $C_1$  and  $L_2$  vary compare with the same as  $C_2$  and  $L_1$  vary. Fig. 3.5 provides graphical representation of stated difference in the rate of change of the eigenfrequencies for for the data as in equations (3.24) and (3.25).*

To get a feel of the considered above perturbation theory let us consider an example consistent with assumptions (3.2) with the following values of the circuit parameters for an EPD point

$$(3.24) \quad \dot{C}_1 = 1, \quad \dot{L}_1 = 1, \quad \dot{C}_2 = -2, \quad \dot{L}_2 = -1,$$

$$\sigma = 1, \quad \delta = -1; \quad \dot{R} = 2\delta\sigma = -2, \text{ for } \dot{g} = g_{-1} = 2 \left(1 - \sqrt{\frac{1}{4}}\right)^2 = \frac{1}{2}.$$

Consequently

$$(3.25) \quad \dot{\xi}_1 = 1, \quad \dot{\xi}_2 = \frac{1}{4}, \quad \dot{\omega}_1 = 1, \quad \dot{\omega}_2 = \frac{1}{4}, \quad \dot{\omega}_0 = \frac{1}{2}.$$

The Figs. 3.1, 3.2, 3.3, 3.4, 3.5, 3.6 and 3.7 show the real and imaginary parts of the four eigenvalues  $s$  as in equations (2.3) assuming that (i) the circuit parameters for the EPD point satisfy equations (3.24) and (3.25); (ii) the perturbed circuit parameters satisfy equations (3.8) where  $\epsilon = 1$  and the eigenvalues approximations to be as in equations (3.12) where we assume  $\epsilon = 1$  and  $\Delta(R)$  is small. One can see in Figure 3.6 that there are exactly two special values of the gyrator parameter  $g$ , namely  $g_{-1} = \frac{1}{2}$  and  $g_1 = \frac{9}{2}$  corresponding to respectively to  $\Delta(g) = 0$  and  $\Delta(g) = 8$ , for which the eigenfrequencies degenerate, see also Fig. Fig. 2.1.

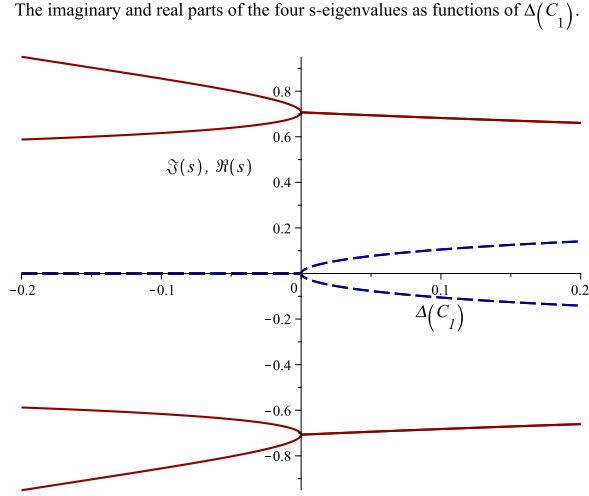
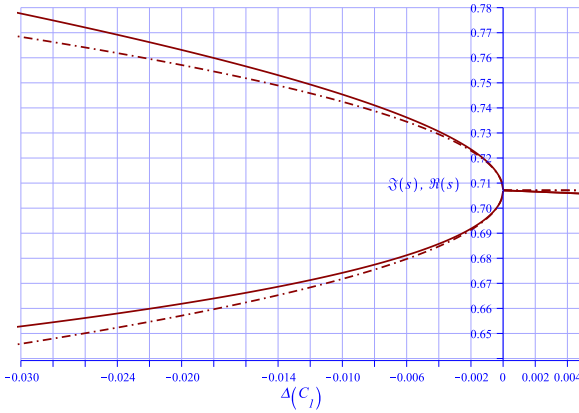


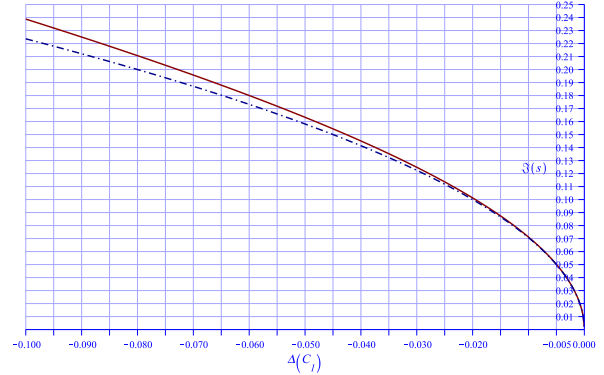
FIGURE 3.1. This plot shows the real (blue dashed line) and imaginary (solid brown line) parts of the four eigenvalues  $s$  as in equations (2.3) assuming that (i) the circuit parameters satisfy equations (3.8) where  $\epsilon = 1$ ,  $\Delta(L_1) = \Delta(L_2) = \Delta(C_2) = \Delta(g) = 0$  and  $\Delta(C_1)$  varies. In other words, the plot shows the variation of the real and imaginary parts of the four eigenvalues  $s$  as function on the capacitance  $C_1$ .

The imaginary parts of the two s-eigenvalues and their approximations as functions of  $\Delta(C_1)$ .



(a)

The difference between the imaginary parts of the two s-eigenvalue vs its approximation as functions of  $\Delta(C_1)$ .



(b)

FIGURE 3.2. This plot (a) is fragment of the plot in Figure 3.1 showing also the imaginary parts of the eigenvalue approximations (dot-dash line) as in equations (3.12) where we assume  $\epsilon = 1$  and  $\Delta(R)$  to be small. The plot (b) shows the difference between the imaginary parts of the eigenvalues as in plot (a) and the corresponding approximation (blue dash-dot line).

#### 4. THE CIRCUIT STABLE OPERATION WHEN CLOSE TO AN EPD

The circuit stable operation is critical to its eigenfrequencies measurements. Using an EPD for enhanced sensitivity poses an immediate challenge when it comes to the stability issue. By the very nature of the eigenfrequency degeneracy the circuit when close to an EPD is only marginally stable at the best. A clear manifestation of the instability is the existence of the circuit eigenvalues (eigenfrequencies)  $s = i\omega$  that have non-zero real part with consequent exponential growth in time when the circuit is in the corresponding eigenstate. Figs. 2.1 and 3.1 provide for graphical

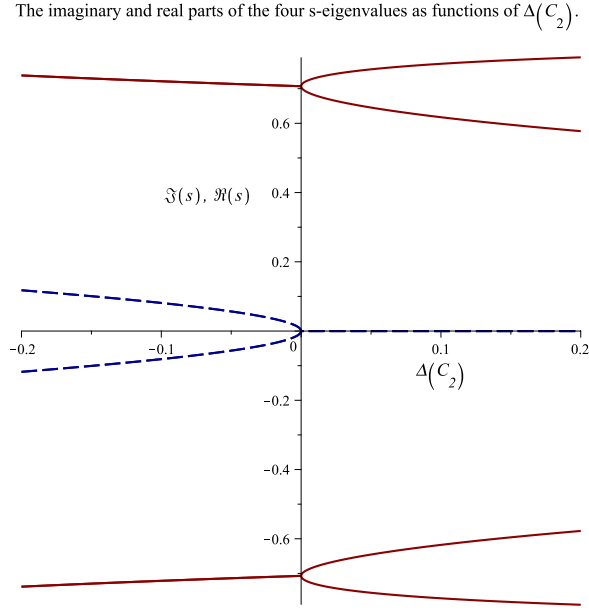
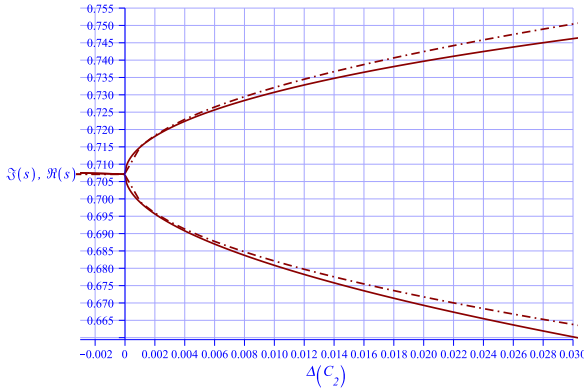


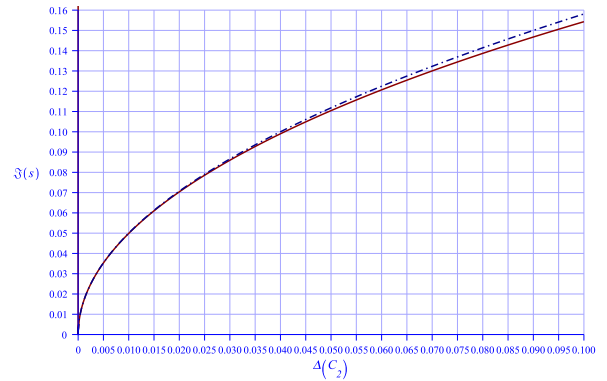
FIGURE 3.3. This plot shows the real (blue dashed curve) and imaginary (solid brown curve) the real and imaginary parts of the four eigenvalues  $s$  as in equations (2.3) assuming that (i) the circuit parameters satisfy equations (3.8) where  $\epsilon = 1$ ,  $\Delta(L_1) = \Delta(L_2) = \Delta(C_1) = \Delta(g) = 0$  and  $\Delta(C_2)$  varies. In other words, the plot shows the variation of the real and imaginary parts of the four eigenvalues  $s$  as function on the capacitance  $C_2$ .

The imaginary of the two s-eigenvalues and their approximations as functions of  $\Delta(C_2)$ .



(a)

The difference between the imaginary parts of the two s-eigenvalue vs its approximation as functions of  $\Delta(C_2)$ .



(b)

FIGURE 3.4. This plot (a) is fragment for the plot in Figure 3.3 showing also the imaginary parts of the eigenvalue approximations (dot-dash line) as in equations (3.12) where we assume  $\epsilon = 1$  and  $\Delta(R)$  to be small. The plot (b) shows the difference between the imaginary parts of the eigenvalues as in plot (a) and the corresponding approximation (blue dash-dot line).

illustration demonstrating the later point. Relations (3.19) and (3.21) make the point on the instability analytically. Indeed, for the data as in equations (3.24) and (3.25) relations (3.19) imply that if  $\frac{C_1 - \hat{C}_1}{C_1} < 0$  then the relative frequency shift  $\frac{\omega_+ - \omega_-}{\omega}$  is real valued and the circuit is stable. But if  $\frac{C_1 - \hat{C}_1}{C_1} > 0$  then the relative frequency shift  $\frac{\omega_+ - \omega_-}{\omega}$  has non-zero imaginary part

The imaginary parts of the two  $s$ -eigenvalues as functions of  $\Delta(C_1), \Delta(C_2)$ .

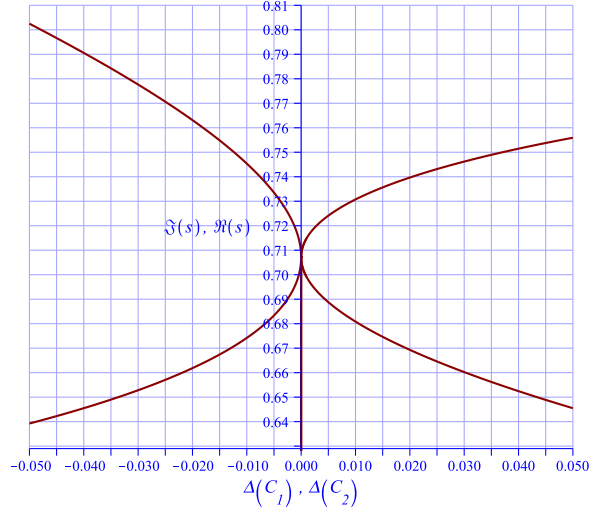


FIGURE 3.5. This plot provides for comparative picture of the variation of the imaginary parts of the eigenvalues shown in Figs. 3.1 and 3.3 as  $\Delta(C_1)$  and  $\Delta(C_2)$  vary. The lines on the left and on the right represent respectively the variation of  $s$  as  $\Delta(C_1)$  and  $\Delta(C_2)$  vary. Notice that the imaginary part of the eigenvalues vary more with variation of  $\Delta(C_1)$  then with variation of  $\Delta(C_2)$  in compliance with equations (3.19) and (3.21) and Theorem 5.

The imaginary and real parts of the four  $s$ -eigenvalues as function of  $\Delta(g)$ .

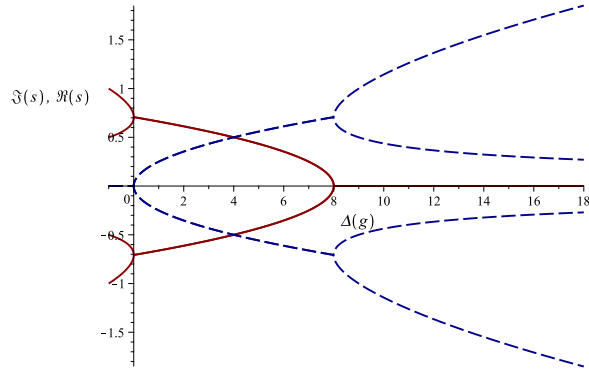


FIGURE 3.6. This plot shows the real (blue dashed curve) and imaginary (solid brown curve) the real and imaginary parts of the four eigenvalues  $s$  as in equations (2.3) assuming that (i) the circuit parameters satisfy equations (3.8) where  $\epsilon = 1$ ,  $\Delta(L_1) = \Delta(L_2) = \Delta(C_1) = \Delta(C_2) = 0$  and  $\Delta(g)$  varies. In other words, the plot shows the variation of the real and imaginary parts of the four eigenvalues  $s$  as function on the capacitance  $g$ .

and consequently the circuit is unstable. This analysis suggest a trade-off approach for combining advantages of employing an EPD point of the circuit for the enhanced sensitivity and the circuit stability. *This trade-off approach is to use as the circuit work point its state close to an EPD but not exactly at it so all the circuit eigenfrequencies are real and consequently its operation is stable. The close proximity to an EPD point should be chosen so that the expected circuit perturbations should reliably maintain the circuit stability.*

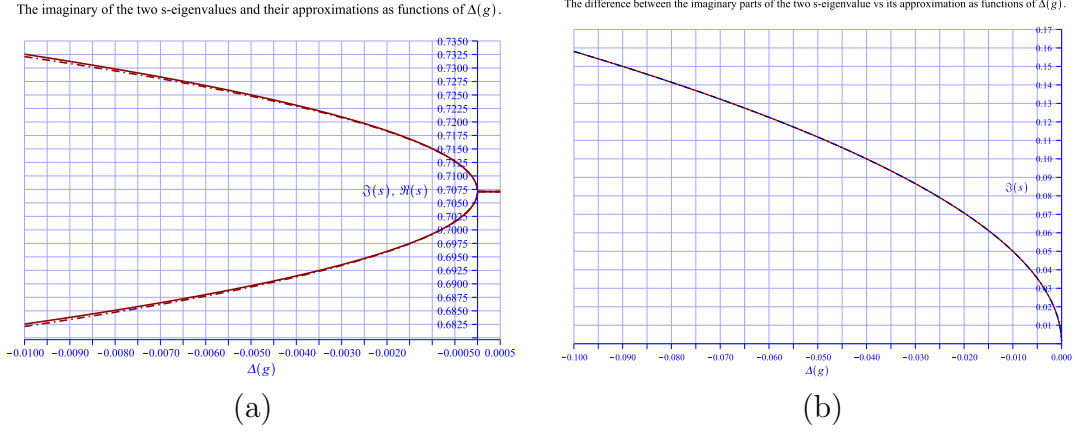


FIGURE 3.7. This plot (a) is fragment for the plot in Figure 3.6 showing also the imaginary parts of the eigenvalue approximations (dot-dash line) as in equations (3.12) where we assume  $\epsilon = 1$  and  $\Delta(R)$  to be small. The plot (b) shows the difference between the imaginary parts of the eigenvalues as in plot (a) and the corresponding approximation (blue dash-dot line). Evidently, the approximation is essentially the same as the difference between the imaginary parts of the eigenvalues.

To quantify the suggested above trade-off between the circuit enhanced sensitivity and its stability we proceed as follows. Suppose that quantity that varies about its EPD value is the capacitance  $C_1$  with understanding that other circuit parameters variation can be treated similarly. Having in mind the relative frequency shift  $\frac{\omega_+ - \omega_-}{\dot{\omega}}$  defined by equation (3.14) let consider its approximation (3.19) for capacitance  $C_1$  varying about its EPD value  $\dot{C}_1$

$$(4.1) \quad \Delta(c) = \sqrt{-ac} \cong \frac{\omega_+ - \omega_-}{\dot{\omega}}, \quad a = \frac{\omega_1}{\omega_2} - 1, \quad c = \Delta(C_1), \quad |c| \ll 1.$$

Notice that if  $ac > 0$  then  $\Delta(c)$  is pure imaginary manifesting the circuit instability. Since we want to assure the circuit stable operation we need to enforce inequality  $ac < 0$ . We achieve that by partitioning  $c$  into two numbers

$$(4.2) \quad c = w + x, \quad aw < 0, \quad |x| \leq \frac{|w|}{2}, \quad |w| \ll 1.$$

Number  $w$  in the partitioning (4.2) is assumed to be chosen and fixed whereas number  $x$  can vary within allowed limit  $|x| \leq \frac{|w|}{2}$  implying inequality  $ac < 0$  and consequently the stability. We refer to number  $w$  as the *work point*. We introduce also the variation function about the work point

$$(4.3) \quad \Delta_w(x) = \Delta(w + x) - \Delta(w) = \sqrt{-a(w + x)} - \sqrt{-aw},$$

and the *enhancement factor function*

$$(4.4) \quad F_w(x) = \left| \frac{\Delta_w(x)}{x} \right| = \left| \frac{\sqrt{-a(w + x)} - \sqrt{-aw}}{x} \right|.$$

Notice that the following asymptotic formulas holds for variation function  $\Delta_w(x)$  defined by equation (4.3)

$$(4.5) \quad \Delta_w(x) = \frac{\sqrt{-aw}}{2w}x - \frac{\sqrt{-aw}}{8w^2}x^2 + \frac{\sqrt{-aw}}{16w^3}x^3 + O(x^4), \quad x \rightarrow 0.$$

Asymptotic expression (4.5) in view of equation (4.2) readily implies the following representation for the enhancement factor function  $F_w(x)$

$$(4.6) \quad F_w(x) = \left| \frac{\sqrt{-aw}}{2w} - \frac{\sqrt{-aw}}{8w^2}x + \frac{\sqrt{-aw}}{16w^3}x^2 + O(x^3) \right|, \quad x \rightarrow 0.$$

*Remark 6* (quantifying trade-off). The expression (4.5) for enhancement factor  $F_w(0)$  and relations (4.2) quantify the trade-off for taking smaller values of  $w$ . Indeed smaller  $w$  yield larger enhancement factor but the stability condition  $|x| \leq \frac{|w|}{2}$  requires constraints the allowed variation of  $x$  to a smaller interval. The indicated trade-off allows to identify the smallest  $w$  acceptable for desired range of values for  $x$ .

Figure 4.1 shows the values of the enhancement factor function  $F_w(x)$  for different values of  $w$  and  $a = \frac{\omega_1}{\omega_2} - 1$ .

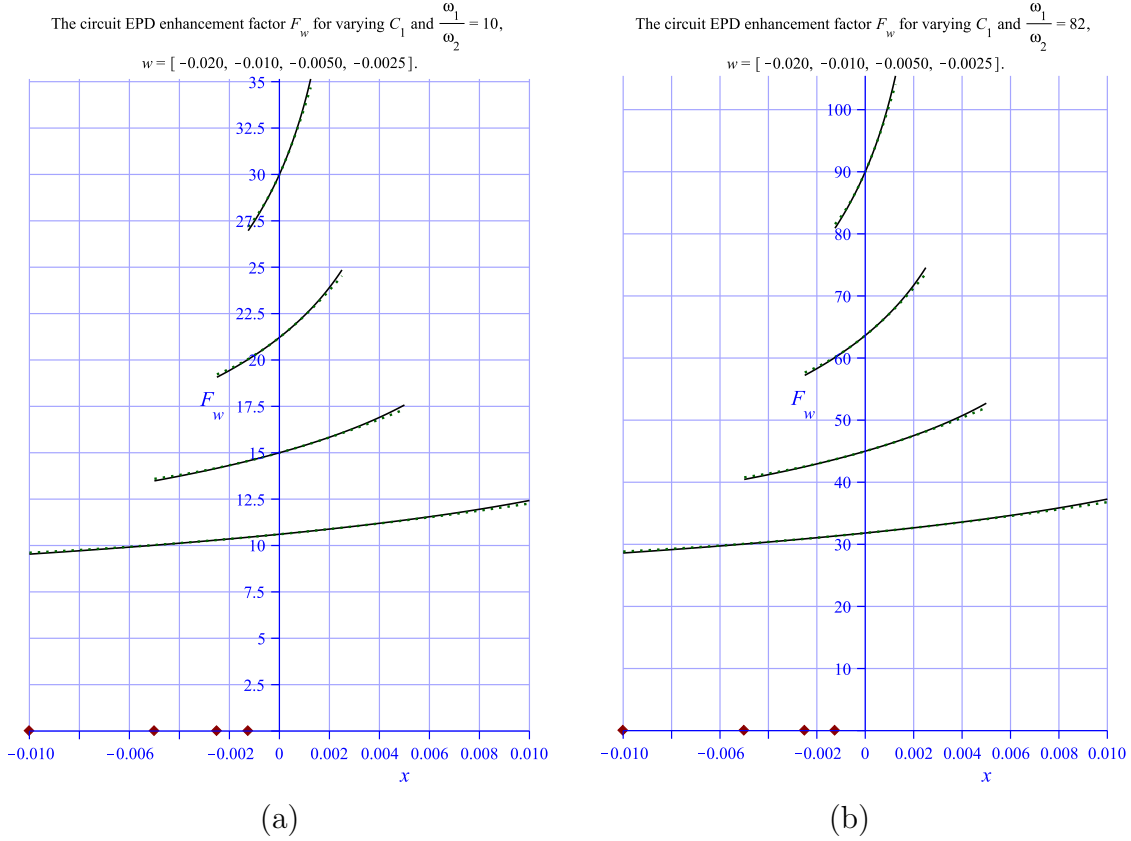


FIGURE 4.1. This plot shows the enhancement factor function  $F_w(x)$  defined in equation (4.5) as solid (black) lines and its approximation as in equation (4.6) as dotted (green) lines for (i) a number of values  $w = -0.02, -0.01, -0.005, -0.0025$ ; (ii) two values  $\frac{\omega_1}{\omega_2} = 10$  for plot (a) and  $\frac{\omega_1}{\omega_2} = 82$  for the plot (b). The variable  $x$  varies in interval  $[-|w|, |w|]$  and the corresponding values of  $w$  are identified on  $x$ -axis by diamond (brown) dots. Smaller values of  $w$  yield larger values of function  $F_w(x)$ . Notice also that the function  $F_w(x)$  approximations fit extremely well its values over indicated intervals.

## 5. A FEW POINTS ON SENSITIVITY OF MEASUREMENTS

Since we pursue here enhanced sensitivity and higher resolution measurements using the circuits described in previous sections we provide a brief review of sensors and their capabilities based on [Bish, 5.3] and references there. Microsensors seems to be the class of sensors particular suited for enhanced sensitivity and higher resolution measurements. According to [Bish, 5.3] they are typically based on either measurement of mechanical strain, measurement of mechanical displacement, or on frequency measurement of a structural resonance. Displacement measurement are often based on the capacitance readout [BoxGre], [Brook], [LeuRud], [Munt], [Seid]. Resonant-type sensors measure frequency and they are generally less susceptible to noise and thus typically provide a higher resolution measurement. These type of sensors provide as much as one hundred times the resolution of analog sensors, though they are more complex and are typically more difficult to fabricate. Using proposed here circuits can enhance the analog sensor sensitivity and resolution by more 100 times making them a competitive alternative to more complex resonant-type sensors.

The reported accuracy of sensors based on (differential) capacitance is 500 ppm (0.05%) with the smallest change in sensed capacitance being about 20 aF, [BoxGre]. As to capacitance tolerances the tolerance values between 1% and 20% are common, and precision capacitor tolerances range from 0.1% to 0.5%, [WhitH, 8.2.3], [WhitE, 2.6.7].

Using frequencies for assessing the circuit related quantities is justified by the fact that time interval and frequency can be measured with less uncertainty and more resolution than any other physical quantity. The accuracy of the low cost frequency counters can be  $1 \times 10^{-7}$  in 1 s, [Bish, 10], [Boye, 27.8]. The current limit for TIC resolution is about 20 ps, which means that a frequency change of  $2 \times 10^{-11}$  can be detected in 1 s [Bish, 10]. Today, the best time and frequency standards can realize the SI second with uncertainties of  $\cong 1 \times 10^{-15}$ .

We remind also that according to the basics of measurement theory the true value of a measured quantity is known only in the case of calibration of measurement instruments [Rab, 1.5]. In this case, the true value is the value of the measurement standard used in the calibration, whose inaccuracy must be negligible compared with the inaccuracy of the measurement instrument being calibrated. If  $x$  is true value of measured quantity and  $\tilde{x}$  is the result of measurement then the absolute error  $\Delta x = \tilde{x} - x$ , and the relative error is  $\delta x = \frac{\tilde{x}-x}{x}$ , [Rab, 1.5].

When equations (4.4) and (4.6) define the enhancement function  $F_w(x)$  and Figure 4.1 shows its values for a range of values of  $x$  we would like to introduce a simpler enhancement characterization as its value at the work point, that is for  $x = 0$ :

$$(5.1) \quad F_w(0) = \frac{\sqrt{|a|}}{2\sqrt{|w|}} = \frac{\sqrt{\left|\frac{\omega_1}{\omega_2} - 1\right|}}{2\sqrt{|w|}}.$$

It turns out that quantity  $F_w(0)$  is relevant to the resolution of measurements at the work point. Indeed, equation (4.1) implies that the resolution  $\rho_x$  for  $x$  at  $x = 0$ , that is at the work point  $w$ , is related to the resolution  $\rho_f$  for the relative frequency  $\frac{\omega_+ - \omega_-}{\bar{\omega}}$  by the following equation

$$(5.2) \quad \rho_f = |\partial_c \Delta(w)| \rho_x.$$

In view of equations (4.1), (4.3), (4.6) and (5.1) the factor  $|\partial_c \Delta(w)|$  in the right-hand side of equation (5.2) satisfies

$$(5.3) \quad |\partial_c \Delta(w)| = |\partial_x \Delta_w(0)| = \left| \frac{\sqrt{-aw}}{2w} \right| = F_w(0) = \frac{\sqrt{\left|\frac{\omega_1}{\omega_2} - 1\right|}}{2\sqrt{|w|}}.$$

Substitution of expression (5.2) for  $|\partial_c \Delta(w)|$  into equation (5.2) yields

$$(5.4) \quad \rho_x = \frac{\rho_f}{F_w(0)} = \frac{2\sqrt{|w|}}{\sqrt{\left|\frac{\omega_1}{\omega_2} - 1\right|}} \rho_f.$$

Figure 5.1 illustrates the dependence of the enhancement factor  $F_w(0)$  on  $w$  and the circuit parameters.

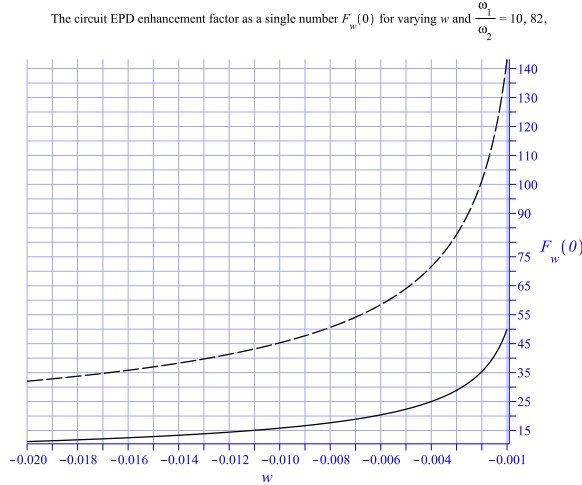


FIGURE 5.1. This plot shows the enhancement factor  $F_w(0)$  defined in equation (5.1) for a range of values of  $w$  and for (a)  $\frac{\omega_1}{\omega_2} = 10$  as solid line; (b)  $\frac{\omega_1}{\omega_2} = 82$  as dashed line. The shown values of  $F_w(0)$  together with formula (5.4) relating resolutions  $\rho_x$  and  $\rho_f$  shows the circuit can enhance the resolution  $\rho_x$  by one or two orders of magnitude.

## 6. JORDAN BLOCKS VIEWED THROUGH THEIR PERTURBATIONS

The determination by numerical evaluations of the presence of nontrivial Jordan blocks in the Jordan canonical form of a matrix is a rather complicated matter. The reason for the problem is that an infinitesimally small perturbation of the matrix can make it completely diagonalizable. An explanation to this seemingly paradoxical situation is that though the perturbed matrix is diagonal some of its relevant eigenvectors are nearly parallel indicating the perturbed matrix proximity to a matrix with nontrivial (non-diagonal) Jordan canonical form. The explanation suggests that a numerically sound determination of the presence of nontrivial Jordan blocks in the Jordan form of a matrix can be based on the matrix perturbations and we pursue this idea here.

The perturbation theory of the matrix Jordan structure in the case of generic perturbations is known as *Lidskii's theory* [Lids], [MoBuOv], [Baum, 7.4], [SeyMai, 2.5], [KirO, 4.4.2]. Lidskii's theory allows to determine effectively the first significant perturbation for the eigenvalues and the Jordan basis vectors. Under additional conditions the theory yields the power series representations for the eigenvalues and the Jordan basis vectors. In the case of nonderogatory (geometric multiplicity one) eigenvalue and a generic perturbation there is constructive recursive algorithm for computing all coefficients for these power series due to Welters [Welt].

Our goal here to develop based on some concepts and results of Lidskii's theory constructive approaches for detecting nontrivial Jordan blocks in the Jordan canonical form of a matrix by their manifestation in the matrix generic perturbations.



Let  $\mathbb{C}^{n \times n}$  be the set of  $n \times n$  matrices with complex-valued coefficients and let matrix  $A \in \mathbb{C}^{n \times n}$ . Consider now a perturbation  $A(\varepsilon)$  of matrix  $A$  of the following form

$$(6.1) \quad A(\varepsilon) = A + B(\varepsilon), \quad B(\varepsilon) = B_1\varepsilon + \sum_{k=2}^{\infty} B_k\varepsilon^k, \quad A, B_k \in \mathbb{C}^{n \times n},$$

where  $\varepsilon$  is a small parameter and the power series is assumed to converge. Suppose now that  $\lambda_0$  is a nonderogatory eigenvalue of the algebraic multiplicity  $m$ , that is its geometric multiplicity is exactly 1. Suppose  $\mathcal{J}$  be the Jordan form of matrix  $A$  and  $Z$  be  $n \times n$  matrix the columns of which form the Jordan basis matrix  $A$ . Then

$$(6.2) \quad \mathcal{J} = Z^{-1}AZ = \begin{bmatrix} J_m(\lambda_0) & 0 \\ 0 & J \end{bmatrix}, \quad J_m(\zeta) = \begin{bmatrix} \zeta & 1 & \cdots & 0 & 0 \\ 0 & \zeta & 1 & \cdots & 0 \\ 0 & 0 & \ddots & \cdots & \vdots \\ \vdots & \vdots & \ddots & \zeta & 1 \\ 0 & 0 & \cdots & 0 & \zeta \end{bmatrix},$$

where  $J$  is the part of the Jordan form  $\mathcal{J}$  related to the eigenvalues of  $A$  different than  $\lambda_0$  and  $J_m(\zeta)$  is the Jordan block of dimension  $m$  associated with eigenvalue  $\zeta$ . Using equations (6.2) we introduce the following matrices represented in block form

$$(6.3) \quad Z^{-1}AZ = \begin{bmatrix} J_m(\lambda_0) & 0 \\ 0 & J \end{bmatrix}, \quad Z^{-1}B_1Z = \begin{bmatrix} \tilde{B}_1 & * \\ * & * \end{bmatrix},$$

where symbol “\*” signifies matrix blocks of relevant dimensions. Let us consider now entries of block  $\tilde{B}_1 \in \mathbb{C}^{m \times m}$

$$(6.4) \quad \tilde{B}_1 = \begin{bmatrix} * & * & \cdots & * & * \\ \vdots & * & * & \cdots & * \\ * & \vdots & \ddots & \cdots & \vdots \\ b_{m-1,1} & * & \ddots & * & * \\ b_{m,1} & b_{m,2} & \cdots & * & * \end{bmatrix},$$

where entries marked by “\*” are of no particular significance.

Let  $\mathbb{C}^n$  be a set of column-vectors with complex-valued entries and let  $e_j$ ,  $1 \leq j \leq n$  be its standard basis. Our first statement will be on the geometric multiplicity  $\text{gmul}_A(\lambda_0)$  of an eigenvalue  $\lambda_0$  of matrix  $A$ . We remind that the geometric multiplicity  $\text{gmul}_A(\lambda_0)$  is defined as the dimension of the eigenspace of matrix  $A$  corresponding to the eigenvalue  $\lambda_0$ . The statement holds under certain genericity assumption and to formulate it we proceed as follows.

Let  $V$  be the eigenspace of matrix  $A$  corresponding to the eigenvalue  $\lambda_0$  and  $W$  be the eigenspace of matrix  $A^*$ , which is adjoint to  $A$ , corresponding to the eigenvalue  $\bar{\lambda}_0$  which is complex-conjugate to  $\lambda_0$ .

$$(6.5) \quad \dim V = \dim W = \text{gmul}_A(\lambda_0) = \text{gmul}_{A^*}(\bar{\lambda}_0) = r.$$

Let

$$(6.6) \quad A_0 = A - \lambda_0\mathbb{I}, \quad U = [u_1, u_2, \dots, u_m, u_{m+1}, \dots, u_n],$$

where matrix  $U \in \mathbb{C}^{n \times n}$  is an orthogonal matrix formed by its column-vectors

$$(6.7) \quad u_j = Ue_j \in \mathbb{C}^n, \quad 1 \leq j \leq n.$$

We suppose now that the first  $r$  column-vectors  $u_j$  are chosen to form an orthonormal basis of the vector space  $V$  and consequently they are eigenvectors of matrix  $A$  corresponding to the eigenvalue  $\lambda_0$ , that is

$$(6.8) \quad A_0 u_j = (A - \lambda_0 \mathbb{I}) u_j = 0, \quad 1 \leq j \leq r.$$

Notice that the general identity  $r + \text{rank} \{A\} = n$  implies that

$$(6.9) \quad A_0 u_j, \quad r + 1 \leq j \leq n, \text{ are linearly independent.}$$

Let matrix  $S \in \mathbb{C}^{n \times n}$  be an invertible matrix such that

$$(6.10) \quad S A_0 u_j = e_j, \quad r + 1 \leq j \leq n,$$

the existence of which is warranted by relations (6.9). In view of (6.7), (6.8) and (6.10) we have

$$(6.11) \quad S A_0 U e_j = 0, \quad 1 \leq j \leq r; \quad S A_0 U e_j = e_j \quad r + 1 \leq j \leq n,$$

and consequently matrix  $S A_0 U \in \mathbb{C}^{n \times n}$  has the following block form

$$(6.12) \quad S A_0 U = \begin{bmatrix} 0 & 0 \\ 0 & \mathbb{I} \end{bmatrix}, \quad A_0 = A - \lambda_0 \mathbb{I},$$

where upper diagonal block matrix  $0 \in \mathbb{C}^{r \times r}$ ,  $\mathbb{I} \in \mathbb{C}^{(n-r) \times (n-r)}$  and off-diagonal block matrices are 0 matrices of the relevant dimensions.

**Theorem 7** (geometric multiplicity test). *Suppose that  $\lambda_0$  is an eigenvalue of matrix  $A \in \mathbb{C}^{n \times n}$  of the geometric multiplicity*

$$(6.13) \quad r = \text{gmul}_A(\lambda_0).$$

Let matrix  $B(\varepsilon) \in \mathbb{C}^{n \times n}$  be represented by converging power series

$$(6.14) \quad B(\varepsilon) = B_1 \varepsilon + \sum_{k=2}^{\infty} B_k \varepsilon^k, \quad B_k \in \mathbb{C}^{n \times n}, \quad 1 \leq k \leq n.$$

Then

$$(6.15) \quad \det \{A + B(\varepsilon) - \lambda_0 \mathbb{I}\} = O(\varepsilon^r).$$

Let matrices  $U$  and  $S$  be as the described before the statement of this theorem. Suppose that matrix  $S B_1 U$  is partitioned conformally with matrix  $S A_0 U$  in (6.12) and is of the following block form

$$(6.16) \quad S B_1 U = \begin{bmatrix} b_1 & * \\ * & * \end{bmatrix},$$

where  $b_1 \in \mathbb{C}^{r \times r}$ . Assume that matrix  $S B_1 U$  satisfies the genericity condition in the form

$$(6.17) \quad \det \{b_1\} \neq 0.$$

Then

$$(6.18) \quad \det \{A + B(\varepsilon) - \lambda_0 \mathbb{I}\} = d \varepsilon^r + O(\varepsilon^{r+1}), \quad d = \frac{\det \{b_1\}}{\det \{S\}} \neq 0, \quad \varepsilon \rightarrow 0.$$

*Proof.* Using block s (6.6).representation (6.16) and equation (6.12) we obtain

$$(6.19) \quad S(A + B(\varepsilon) - \lambda_0 \mathbb{I})U = S(A_0 + B(\varepsilon))U = \begin{bmatrix} b_1 \varepsilon + O(\varepsilon^2) & O(\varepsilon) \\ O(\varepsilon) & \mathbb{I} + O(\varepsilon) \end{bmatrix}, \quad \varepsilon \rightarrow 0.$$

Then applying equation (7.3) of Proposition 10 to the block matrix in the right-hand side of equations (6.19)

$$(6.20) \quad \det \{S(A + B(\varepsilon) - \lambda_0 \mathbb{I})U\} = \varepsilon^r \det \{b_1\} + O(\varepsilon^{r+1}), \quad \varepsilon \rightarrow 0.$$

Since  $U$  is an orthogonal matrix  $\det U = 1$  equation (6.20) readily implies relations (6.15) and (6.18).  $\square$

The presence of a nontrivial Jordan block in the Jordan form of a matrix  $A$  can be detected in a number of ways based on its perturbation  $A(\varepsilon) = A + B(\varepsilon)$ . The following statement due to Welters, [Welt], establishes the equivalency of some of those ways.

**Proposition 8** (perturbation of nonderogatory eigenvalue). *Let  $A(\varepsilon)$  be  $\mathbb{C}^{n \times n}$  matrix-valued analytic function of  $\varepsilon$  for small  $\varepsilon$ . Let  $\lambda_0$  be an eigenvalue of the unperturbed matrix  $A(0)$  of the algebraic multiplicity  $m$ . Then the following statements are equivalent:*

- (i) *The characteristic polynomial  $\det \{\lambda \mathbb{I} - A(\varepsilon)\}$  has a simple zero with respect to  $\varepsilon$  at  $\lambda = \lambda_0$  and  $\varepsilon = 0$ , that is*

$$(6.21) \quad \frac{\partial}{\partial \varepsilon} \det \{\lambda \mathbb{I} - A(\varepsilon)\} \Big|_{(\varepsilon, \lambda) = (0, \lambda_0)} \neq 0.$$

- (ii) *The characteristic equation  $\det \{\lambda \mathbb{I} - A(\varepsilon)\} = 0$  has a unique solution,  $\varepsilon(\lambda)$ , in a neighborhood of  $\lambda = \lambda_0$  with  $\varepsilon(\lambda_0) = 0$ . This solution is an analytic function with a zero of order  $m$  at  $\lambda = \lambda_0$ , i.e.,*

$$(6.22) \quad \varepsilon(\lambda_0) = \frac{d\varepsilon(\lambda)}{d\lambda} \Big|_{\lambda=\lambda_0} = \dots = \frac{d^{m-1}\varepsilon(\lambda)}{d\lambda^{m-1}} \Big|_{\lambda=\lambda_0} = 0, \quad \frac{d^m\varepsilon(\lambda)}{d\lambda^m} \Big|_{\lambda=\lambda_0} \neq 0.$$

- (iii) *There exists a convergent Puiseux series whose branches are given by*

$$(6.23) \quad \lambda_h(\varepsilon) = \lambda_0 + \alpha_1 \zeta^h \varepsilon^{\frac{1}{m}} + \sum_{k=2}^{\infty} \alpha_k \left( \zeta^h \varepsilon^{\frac{1}{m}} \right)^k, \quad h = 0, \dots, m-1, \quad \zeta = e^{\frac{2\pi i}{m}},$$

*for any fixed branch of  $\varepsilon^{\frac{1}{m}}$ , and the first order term is nonzero, i.e.,*

$$(6.24) \quad \alpha_1 \neq 0.$$

*The values of the branches  $\lambda_h(\varepsilon)$  give all the solutions of the characteristic equation for sufficiently small  $\varepsilon$  and  $\lambda$  sufficiently near  $\lambda_0$ .*

- (iv) *The Jordan normal form of  $A(0)$  corresponding to the eigenvalue  $\lambda_0$  consists of a single  $m \times m$  Jordan block, and there exists an eigenvector  $u_0$  of  $A(0)$  corresponding to the eigenvalue  $\lambda_0$  and an eigenvector  $v_0$  of matrix  $A^*(0)$  (adjoint to  $A(0)$ ) corresponding to the eigenvalue  $\bar{\lambda}_0$  such that*

$$(6.25) \quad (v_0, B_1 u_0) \neq 0, \quad B_1 = \frac{dA(\varepsilon)}{d\varepsilon} \Big|_{\varepsilon=0}.$$

One of the ways to utilize Proposition 8 for detecting a Jordan block in the Jordan form of a matrix  $A$  is to establish numerically that the perturbed matrix  $A + B(\varepsilon)$  has eigenvalues consistent with the Puiseux series (6.23) involving fractional power  $\varepsilon^{\frac{1}{m}}$ . That would allow to claim that the the Jordan normal form of  $A(0)$  corresponding to the eigenvalue  $\lambda_0$  consists of a single  $m \times m$  Jordan block.

An alternative way to detect the presence of a Jordan block associated with  $A$  is to utilize the statement (ii) of Proposition 8. Namely, one can try to establish numerically that there is a unique solution  $\varepsilon(\lambda)$  to characteristic equation  $\det \{\lambda \mathbb{I} - A(\varepsilon)\} = 0$  in the vicinity of  $\varepsilon = 0$  and  $\lambda = \lambda_0$  which is consistent with the following equations

$$(6.26) \quad \frac{\varepsilon(\lambda)}{(\lambda - \lambda_0)^m} = c_1 + O((\lambda - \lambda_0)), \quad c > 0, \quad \lambda \rightarrow \lambda_0,$$

where  $m$  is a positive integer. If the relation (6.26) for  $\varepsilon(\lambda)$  is established it would imply that the the Jordan normal form of  $A(0)$  corresponding to the eigenvalue  $\lambda_0$  consists of a single  $m \times m$  Jordan block.

There is yet another useful statement for verifying that the Jordan form of matrix  $A$  has a nontrivial Jordan block. To formulate it we introduce the following operator norm on the set of matrices  $\mathbb{C}^{n \times n}$ :

$$(6.27) \quad \|A\|_\infty = \max_{1 \leq j \leq n} \left\{ \sum_{i=1}^n |a_{ij}| \right\}, \quad A = \{a_{ij}\}_{i,j=1}^n,$$

where  $i$  and  $j$  are respectively the row the column indexes. Here is the statement due Bauer and Fike [HorJohn, 6.3].

**Proposition 9** (perturbation of a diagonalizable matrix). *Let  $A$  be  $\mathbb{C}^{n \times n}$  matrix which is diagonalizable, that is  $A = SAS^{-1}$ , in which  $S$  is nonsingular and  $\Lambda$  is diagonal. Let  $B$  be  $\mathbb{C}^{n \times n}$  matrix. If  $\tilde{\lambda}$  is an eigenvalue of  $A + B$ , there is an eigenvalue  $\lambda$  of  $A$  such that*

$$(6.28) \quad \left| \tilde{\lambda} - \lambda \right| \leq \kappa_\infty(S) \|B\|_\infty, \quad \kappa_\infty(S) = \|S\|_\infty \|S^{-1}\|_\infty,$$

in which  $\kappa_\infty(S)$  is the co-called condition number with respect to the norm  $\|\cdot\|_\infty$ .

A way to utilize Proposition 9 is to consider perturbed matrix  $A + B(\varepsilon)$  and establish numerically that  $\left| \tilde{\lambda} - \lambda \right| > c\varepsilon^\alpha$  where  $c > 0$  and  $0 < \alpha < 1$ . Then since the indicated inequality involves fractional power  $\varepsilon^\alpha$  with  $0 < \alpha < 1$  it would be inconsistent with inequality (6.28) where  $\|B(\varepsilon)\|_\infty = |\varepsilon| \|B\|_\infty$  implying that unperturbed matrix  $A$  can not be diagonalized, and consequently that the Jordan form of  $A$  has to have a nontrivial Jordan block.

## 7. APPENDIX

**7.1. Appendix B: Some properties of block matrices.** The statements on block matrices below are useful for our studies [BernM, 2.8].

**Proposition 10** (factorization of a block matrix). *Let  $A \in \mathbb{C}^{n \times n}$ ,  $B \in \mathbb{C}^{n \times m}$ ,  $C \in \mathbb{C}^{p \times n}$ ,  $D \in \mathbb{C}^{p \times m}$ , and assume  $A$  is nonsingular. Then*

$$(7.1) \quad \begin{bmatrix} A & B \\ C & D \end{bmatrix} = \begin{bmatrix} I & 0 \\ CA^{-1} & I \end{bmatrix} \begin{bmatrix} A & 0 \\ 0 & D - CA^{-1}B \end{bmatrix} \begin{bmatrix} I & A^{-1}B \\ 0 & I \end{bmatrix},$$

and

$$(7.2) \quad \text{Rank} \left\{ \begin{bmatrix} A & B \\ C & D \end{bmatrix} \right\} = n + \text{Rank} \{D - CA^{-1}B\}.$$

If furthermore,  $m = p$ , that is  $A \in \mathbb{C}^{n \times n}$ ,  $B \in \mathbb{C}^{n \times m}$ ,  $C \in \mathbb{C}^{m \times n}$ ,  $D \in \mathbb{C}^{m \times m}$ , then[FukSha, 26]

$$(7.3) \quad \det \left\{ \begin{bmatrix} A & B \\ C & D \end{bmatrix} \right\} = \det \{A\} \det \{D - CA^{-1}B\}.$$

**7.2. Joukowski transform.** Joukowski (Zhukovsky) transform, [FukSha, 26], [Simon C2A, 8.4], is defined by

$$(7.4) \quad u = z + \frac{1}{z}.$$

The inverse to it is of the degree 2, that is there are two solutions  $z$  to the equation (7.4) for  $z$ , namely

$$(7.5) \quad z_1 = \frac{u - \sqrt{u^2 - 4}}{2}, \quad z_2 = \frac{u + \sqrt{u^2 - 4}}{2} = \frac{1}{z_1}.$$

The branch of  $\sqrt{u^2 - 4}$  in equations (7.5) is defined so that  $\sqrt{u^2 - 4} = u\sqrt{1 - \frac{4}{u^2}}$  where the continuous branch of the square root  $\sqrt{1 - \frac{4}{u^2}}$  outside interval  $[-2, 2]$  is chosen by the condition that for  $u = \infty$  we have  $\sqrt{1} = 1$ . For detailed description of the Riemann surface associated with function  $u = z + \frac{1}{z}$  and its inverse function branches in equations (7.5) see [FukSha, 26].

The Joukowski transform  $u = z + \frac{1}{z}$  provides for one-to-one correspondence between the unit disk  $\mathbb{D} = \{z : |z| < 1\}$  and set  $\hat{\mathbb{C}} \setminus [-2, 2]$  where  $\hat{\mathbb{C}} = \mathbb{C} \cup \{\infty\}$ , that is the set of complex numbers  $\mathbb{C}$  extended by adding to it  $\infty$ . The first equation in (7.5) is the inverse to this one-to-one correspondence. The Joukowski transform  $u = z + \frac{1}{z}$  is also one-to-one mapping between (i) the exterior  $\{z : |z| > 1\}$  of the unit disk and (ii) set  $\hat{\mathbb{C}} \setminus [-2, 2]$ . The second equation in (7.5) is the inverse to it. Fig. 7.1 shows the polar orthogonal grid of the unit circle and corresponding under Joukowski transform  $u = z + \frac{1}{z}$  the orthogonal grid on the set  $\hat{\mathbb{C}} \setminus [-2, 2]$ . Notice also the image of

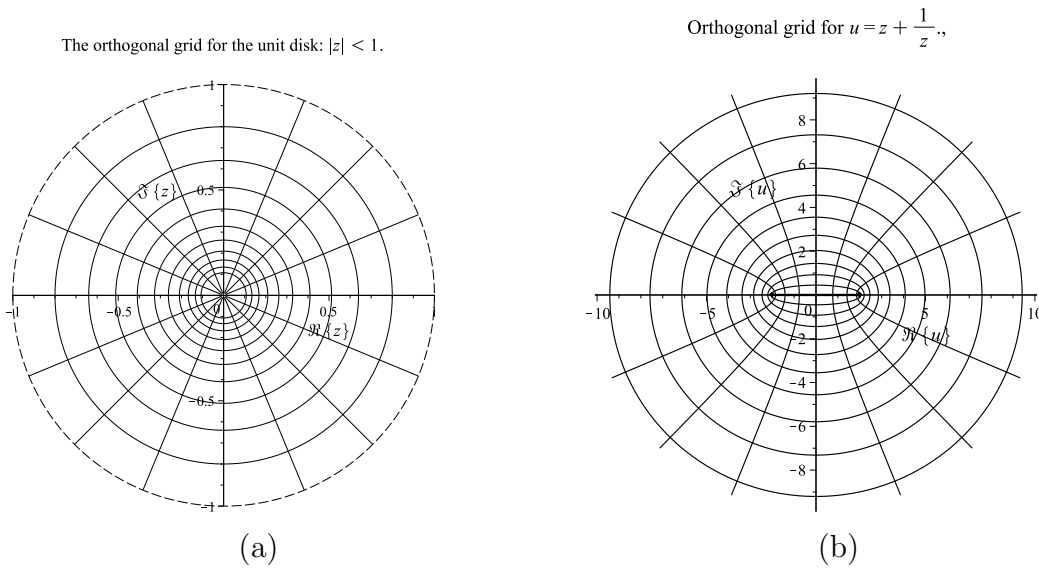


FIGURE 7.1. Plot (a) shows the polar-coordinate grid for the unit disk  $\mathbb{D} = \{z : |z| < 1\}$ . Plot (b) shows the corresponding under Joukowski transform  $u = z + \frac{1}{z}$  the orthogonal grid on the set  $\hat{\mathbb{C}} \setminus [-2, 2]$ . In particular, counterclockwise oriented circles are mapped onto clockwise oriented ellipses as described by relations (7.6).

the circle  $|z| = r < 1$  oriented counterclockwise under Joukowski transform is an ellipse oriented clockwise, namely [FukSha, 26],

$$(7.6) \quad z = r \exp \{i\theta\} \rightarrow u = \frac{1}{2} \left( r + \frac{1}{r} \right) \cos \theta + i \frac{1}{2} \left( r - \frac{1}{r} \right) \sin \theta.$$

The circle  $|z| = 1$  is mapped onto the doubled segment  $[-2, 2]$  with points  $-1$  and  $1$  mapped respectively on  $-2$  and  $2$ . We can think of the upper semi-circle as mapped on the the lower edge of the cut  $[-2, 2]$ , and we think of the lower semi-circle as mapped on the the upper edge of this cut.

**Acknowledgment:** This research was supported by AFOSR grant # FA9550-19-1-0103 and Northrop Grumman grant # 2326345.

REFERENCES

[ArnODE] Arnold V., *Ordinary Differential Equations*, 3rd ed., Springer, 1992. 1

- [Baum] Baumgartel H., *Analytic Perturbation Theory for Matrices and Operators*, Birkhauser, 1985. 6
- [BernM] Bernstein D., *Matrix Mathematics: Theory, Facts, and Formulas*, 2 edn., Princeton University Press, 2009. 7.1
- [Bish] Bishop R., *Mechatronics - an introduction*, CRC, 2006. 5
- [Boye] Boyes W., *Instrumentation reference book*, 4th edition, Elsevier, 2010. 5
- [BoxGre] Boxenhorn B. and Greiff P., *Monolithic silicon accelerometer*, Sensors and Actuators, A21-A23, 273-277 (1990). 5
- [Brook] Brookhuis R. et.al., *Six-axis force-torque sensor with a large range for biomechanical applications*, Jour. of Micromechanics and Microengineering, **24**, 035015, (2014). 5
- [CheN] Chen W. et. al., *Exceptional points enhance sensing in an optical microcavity*, Nature, **548**, 192-196, (2017). 1
- [FigSynbJ] Figotin A., *Synthesis of lossless electric circuits based on prescribed Jordan forms*, arxiv 2020. 1, 2, 2
- [FukSha] Fuks B. and Shabat B., *Functions of a Complex Variable and Some of Their Applications*, vol.1, Pergamon Press, 1961. 10, 7.2, 7.2, 7.2
- [Hale] Hale J., *Ordinary Differential Equations*, 2nd ed., Krieger Publishing Co., 1980. 1
- [HHWGECK] Hodaei H., Hassan A., Wittek S., Garcia-Gracia H., El-Ganainy R., Christodoulides D and M. Khajavikhan, *Enhanced sensitivity at higher-order exceptional points*, Nature, **548**, 187 (2017). 1
- [HorJohn] Horn R. and Johnson C., *Matrix Analysis*, 2nd ed., Cambridge University Press, 2013. 1, 6
- [Kato] Kato T., *Perturbation theory for linear operators*, Springer 1995. 1
- [KirO] Kirillov O., *Nonconservative Stability Problems of Modern Physics*, De Gruyter, 2013. 6
- [KNAC] Kazemi H., Nada M., Mealy T., Abdelshafy A. and Capolino F., *Exceptional Points of Degeneracy Induced by Linear Time-Periodic Variation*, Phys. Rev. Applied, **11**, 014007 (2019). 1
- [LeuRud] Leuthold H. and Rudolf F., *An ASIC for high-resolution capacitive microaccelerometers*, Sensors and Actuators, A21-A23, 278-281 (1990). 5
- [Lids] Lidskii V., *Perturbation theory of non-conjugate operators*, USSR Comput. Math. Math. Phys., **6**, 73-85, (1966). 6
- [MoBuOv] Moro J., Burke J., and Overton M., *On the Lidskii-Vishik-Lyusternik perturbation theory for eigenvalues of matrices with arbitrary Jordan structure*, SIAM J. Matrix Anal. Appl., **18**, 793-817, (1997). 6
- [Munt] Muntwyler S. et.al., *Three-axis micro-force sensor with sub-micro-Newton measurement uncertainty and tunable force range.*, Jour. of Micromechanics and Microengineering, **20**, 025011, (2010). 5
- [PeLiXu] Peng C., Li Z., and Xu A., *Rotation sensing based on a slow-light resonating structure with high group dispersion*, Appl. Opt., **46**, 4125 (2007). 1
- [Rab] Rabinovich S., *Evaluating Measurement Accuracy*, 3rd ed., Springer, 2017.. 5
- [Seid] Seidel H. et.al., *Capacitive silicon accelerometer with highly symmetrical design*, Sensors and Actuators, A21-A23, 312-315, (1990). 5
- [Simon C2A] Simon B., *Basic Complex Analysis. A Comprehensive Course in Analysis*, part 2A, AMS, 2015. 7.2
- [SeyMai] Seyranian A. and Mailybaev A., *Multiparameter Stability Theory with Mechanical Applications*, World Scientific, 2004. 6
- [Wie] Wiersig J., *Enhancing the Sensitivity of Frequency and Energy Splitting Detection by Using Exceptional Points - Application to Microcavity Sensors for Single-Particle Detection*, Phys. Rev. Lett., **112**, 203901 (2014). 1
- [Welt] Welters A., *On explicit recursive formulas in the spectral perturbation analysis of a Jordan Block*, SIAM J. Matrix Anal. Appl., **32**(1), 1-22, (2011). 6, 6
- [WhitH] Whitaker J., *The Resource Handbook of Electronics*, CRC, 2000. 5
- [WhitE] Whitaker J., *The electronics handbook*, CRC 2005. 5
- [Wiel] Wiersig J., *Sensors operating at exceptional points: General theory*, Phys. Rev. A, **93**, 033809 (2016).